HUNGARIAN AGRICULTURAL ENGINEERING
No 41/2022 24-37
Published online: http://hae-journals.org/
HU ISSN 0864-7410 (Print)
HU ISSN 2415-9751(Online)
DOI: 10.17676/HAE.2022.41.24
Received: 30.04.2022 - Accepted: 25.05.2022

PERIODICAL
OF THE COMMITTEE OF AGRICULTURAL AND BIOSYSTEM ENGINEERING OF THE HUNGARIAN ACADEMY OF SCIENCES
and
HUNGARIAN UNIVERSITY OF AGRICULTURE AND LIFE SCIENCES
INSTITUTE OF TECHNOLOGY

DEHYDRATING USING COMBINED ENERGY INTAKE METHOD

Author(s):
V. Madár[1], J. Gubó[2], L. Tóth[3]

Affiliation:
[1] PYROWATT Co. Ltd.,6120 Kiskunmajsa, Vágóhid u. 91., Hungary;
[2] CSŐ-MONTAGE Co. Ltd.; 1103 Budapest, Gyömrői u 33., Hungary;
[3] Institute of Technology - Hungarian University of Agriculture and Life Sciences, 2100 Gödöllő, Páter Károly u. 1., Hungary;

Email address:
madar.viktor@pyrowatt.hu; Gubo.Janos@csomontage.hu; Toth.Laszlo.emeritus@uni-mate.hu

Abstract: Our paper introduces the research and development of a new, continuously operational food dehydrator, and the prototype of said machine. Conditions related to heating technology are required for dehydrators that prevent the vegetables and fruits from suffering too much damage to their internal components. In the new system, traditional convective heat transfer was combined with microwave dehydration, which is well-known for its better efficiency. The final goal is to create an industrial system that can satisfy both small works and industrial demands, while being more energy efficient than traditional solutions, and has faster dehydration potential. However, at the same time, due to dehydrating on lower temperature, it should end up in a gentler drying process. It is fundamental to keep the valuable components of the products intact. The system is continuously operational. The material is sent via conveyor belt through the canal, while magnetrons are operating, and low- heat and moisture airflow is moving above it. Materials dried with the machine were evaluated by the Institute of Horticulture, at the Hungarian University of Agriculture and Life Sciences s (MATE).

Keywords: fruit drying, low-impact drying, microwave, convective energy, energy conservation

1. Introduction

There is a wide array of positive feedback on various foodstuffs forums relating to the advantages of dried and dehydrated fruits and vegetables. Drying, or dehydration are similar processes physically, one of them is the oldest form of conservation (Radu et al., 2018). Both processes deal with the removal of the material's initial high moisture content. The moisture content related from drying is ~12-14% of the original, average moisture content, or even lower. For dehydration, the moisture content is somewhere between 18% and 22%. Fundamental processes have long-standing traditions, they may be extremely simple, or more complex variations.

Apart from conservation, dehydration's purpose is to keep taste- and aroma intact, meaning the enjoyment factor during consumption should remain. Drying and dehydration was done in direct sunlight, when weather conditions were favourable. Even to this day, many consider the dehydration using sunlight the most advantageous. In order to reach sufficient quality, several important factors are necessary: protection from dust, various insects, but damage may come from too strong a sunlight as well, f.e. overheated materials have their colours changed, and their surface hardens. The duration of dehydrating, and the state of the environment (temperature, airflow, air moisture content) where dehydrating is conducted, are also important. The applicable periods for fruits that ripen later are even less, especially in temperate climate, due to frequent and significant changes. As such, most recommend closed- or semi-closed dehydration processes, and dehydrators using electric heating. Removal of hydration can traditionally be done via two processes: convective and conductive heat transfer.

Both processes are known for starting the heating of material on the outside surface, and heat energy is transferring towards the inside (Beke, 1999). Airflow is advantageous for the drying method using sunlight as well, as water and moisture on the surface of the material is transferred through it, away from the material.

Therefore, water (vapour) expelled from the material by the conductive heat flowing into it is realised through a convective method (through airflow), which also makes the process faster. As an example, when conducting dehydration using an oven, it's often advised to slightly open the oven door. Through the opening, air filled with moisture and vapour can exit from the oven, helping and hastening the drying process.

In the earliest larger closed dehydrators, a convective and conductive combination process was used, usually by pouring in hot, dry air. For these processes, energy becomes a significant cost factor. Therefore, one of the goals of these processes is to reduce the energy committed to the process. This should be achieved in a way that doesn't impact the material quality of the end product.

2. Development goals

We have developed a process which aids both energy conservation and quality conservation (Aboltins-Palabinskis, 2018). To reach this goal, we implemented a combination of convective moisture extraction (could be called convective drying), and short wave energy transmission (heat transfer). Short wave heating and cooking has become mainstream nowadays, due to the massive popularity of the microwave oven. There were many debates on its effect on life, and even today, there are many against it. However, nobody could reliably prove that it causes any sort of sickness by itself. If we analyse the physics of the process, we can't find a phenomenon that could support these claims (Radu et al., 2018).

We have designed a machine in which the moisture within the materials is heated swiftly through applying microwaves, and expended in a shorter time towards the surface of the material. From there, the low temperature and vapour content airflow transfers it to the outside. The design of the system can be seen on Fig. 1.

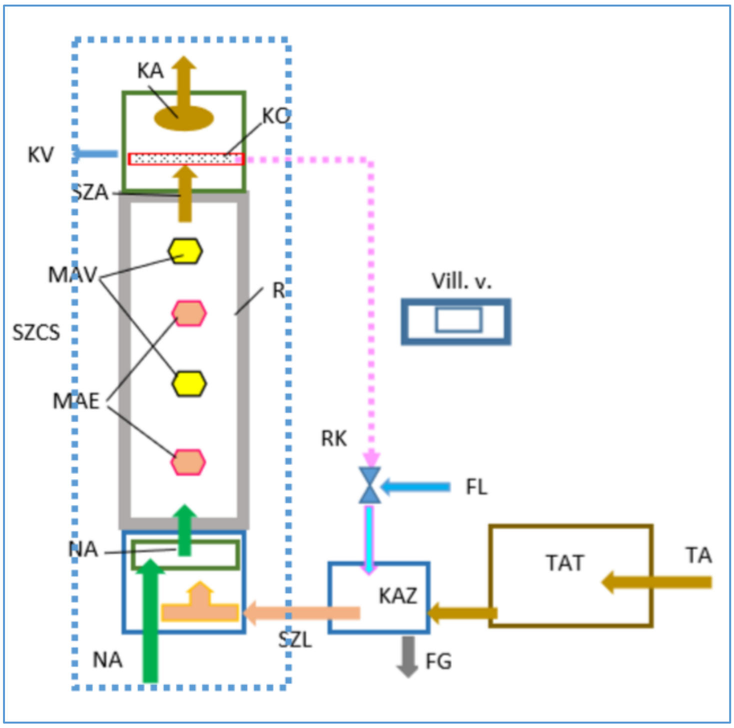

Explanation of abbreviations on the figure:
SZCS – drying channel,
MAV – magnetrons,
MAE – rectified magnetron,
NA – moist material input,
R – cavity resonator,
SZ – dry material,
KA – finished material,
KO – condensator,
KV – waste water,
SZL – dry air input,
KAZ – convection furnace
FG – waste gas,
RK – fresh recuperation air,
TAT – container space,
TA – fuel,
Vill.v – electric control.

Figure 1. Theoretical design of the experimental machine within the closed metal container.

We planned a so-called dehydration tunnel (drying channel) for the system, where the material transferred through perforated conveyor belt undergoes microwave treatment, while a low-temperature and vapour content airflow consistently remains in its direct proximity.

Air flows through the channel (tunnel) above the product on top of the conveyor belt, towards the open end (Fig. 2).

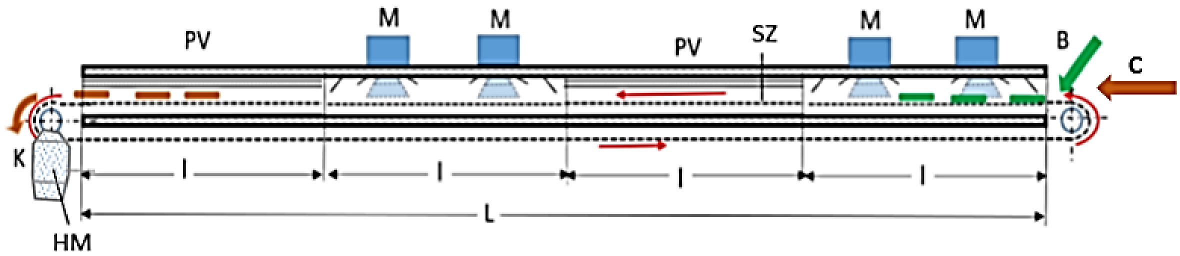

Figure 2. Structure of the tunnel

Explanation of abbreviations on the figure:
M – magnetrons, PV – polarised, high voltage areas, B – input of moist product, C – input of drying airflow, K – end product, measurement, SZ – conveyor belt using plastic belt, HM – engine motor operating the transport conveyor

3. Movement and role of the drying airflow

In convective drying, the most important function belongs to the low moisture/vapour content airflow, which transfers heat into the drying system, heats the materials to dry present within, and extracts the moisture content from the system. (Beke et al, 1999) The total pressure of this moist air (p) comes from the partial pressure of vapour (p_g) and dry air (p_1):

$$p = p_1 + p_g$$

Partial steam pressure:

$$p_g = p\frac{m_g R_g}{mR}$$

where: m_g – mass of the vapour
m – sum of dry air and vapour mass

$$m = m_1 + m_g$$

moisture content of the airflow:

$$x = \frac{m_g}{m_1}$$

Partial pressures can also be used to express the *moisture content of saturated airflow*:

$$x = 0{,}622\frac{p_g}{p - p_g}$$

Relative moisture content, from partial gas pressures:

$$\varphi = \frac{p_g}{p_{gt}}$$

where p_{gt} – gas pressure of saturated airflow.

Evaporation heat is necessary for the evaporation of the material's moisture content. It is only valid for specific moisture content and temperature, as partial gas pressure means the ratio between capillary water and free fluid evaporation. This means that it's *varied, depending on material types and moisture content.* It is always higher than one (Szabó, 2005). This shows that in order to remove capillary water from the materials, more energy is required than necessary for evaporating them from an open surface.

The goal is to affect the capillary water within the material using the microwave, since it is harder to remove (Beke- Mujumdar, 1997).

We mentioned that extracting the moisture from the material's surface is done using the airflow. Therefore, during the aerotechnical analysis, it's important to determine the moist air's enthalpy. In order to do this, Mollier's enthalpy moisture content, also known as i-x diagram is usable (Fig. 3).

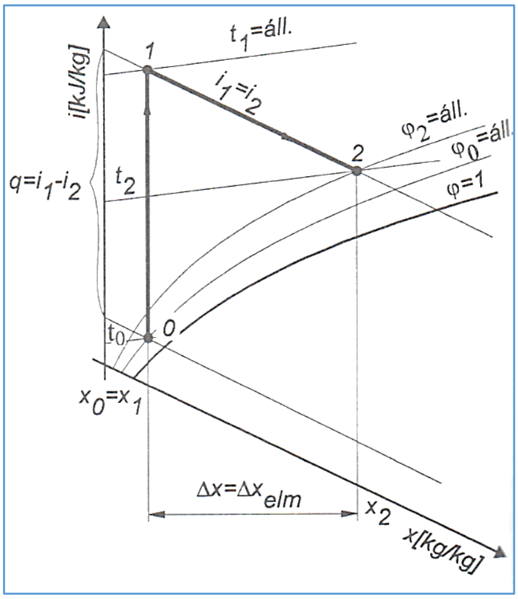

Figure 3. Drying process (Beke, 1997).

The machinery planned for manufacture will be a so-called cross-weighing system, continuously operating. Therefore, calculations have to take this into consideration (Chen et al., 2017), (Janowicz-Lenart, 2018).

During one unit of time, $G_1(kg/h)$ moist material enters the drying area, which has a moisture content of w_1, and a temperature of t_1'. At the end of the drying process, $G_2\ (kg/h)$ of dried material leaves the system at w_2 moisture content and t_2' temperature (Moreno et al., 2018), (Saravacos et al., 1999).

Mass flow of the dried material:

$$G_2 = G_1 \frac{1 - w_1}{1 - w_2} \quad (kg/h)$$

Material balance of evaporated and extracted vapour:

$$W = G_1 - G_2 \qquad (kg/h)$$

For both dry and moist materials:

$$W = G_1 \cdot \frac{w_1 - w_2}{100 - w_2}; \quad W = G_2 \cdot \frac{w_1 - w_2}{100 - w_1}$$

Dehydration potential of the drying airflow W (kg/h):

$$W = L \cdot \Delta x \qquad (kg/h)$$

Where: $\Delta x = (x_2 - x_1)$ g/kg, equals the airflow's moisture intake.
L = airflow volume (kg/h)

Necessary heating performance of the dehydrator Q (MJ/h):

$$Q = L \cdot \Delta i$$

Where: L – volume of drying airflow (kg/h)
$\Delta i = (i_2 - i_1)$ change in heat content (enthalpy) ($kJ/kg_{sz.lev.}$)

Necessary heat performance:

$$Q_h = G_{tü}\, H \qquad (MJ/h)$$

Where: $G_{tü}$ – fuel quantity (kg/h)
H – heat performance of fuel used for the heating process (MJ/kg)

Points of separation on the drying curve can be differentiated by A; B; C; D and E. (Fig. 4)

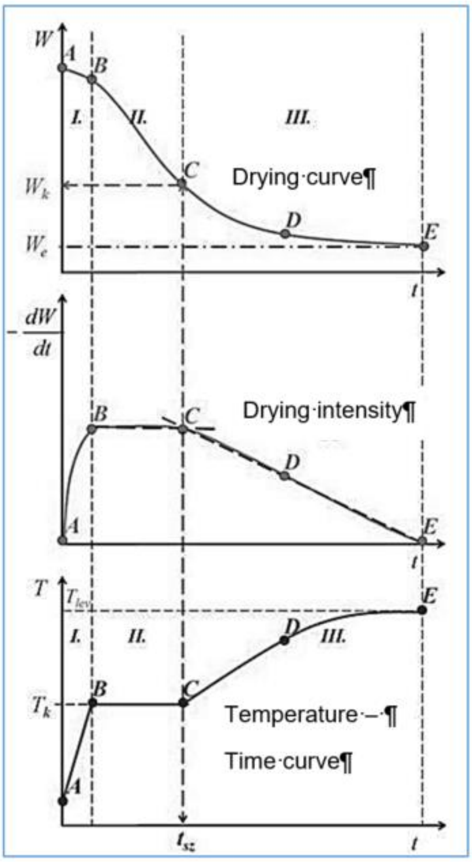

Figure 4. Specific phases of dry (Dévay, 2013)

Explanation of abbreviations on the figure:
I. warming phase; II. constant speed phase; III. decreasing speed phase.

According to experiences (and literature sources), the speed and temperature of the airflow has a significant impact on the colouring. This is why the effects of temperature and air velocity have to be considered. Preparation is necessary for making them variable (Beke, 1999), (Miller et al., 2012).

In general, even changes in the internal components is dependent on the level of heat transmission, since heat level affects various chemical reactions, which are f.e. causes for loss in internal component, and even *aroma*.

For example, the so-called convective drying (dehydration) using airflow, by increasing the speed of dehydrating fruits, loss in aroma also increases. In the case of vegetables and fruits, apart from aroma, proteins, sugars, vitamins, acids and carbohydrates are also damaged.

Nowadays' practice mostly considers the convective process (using airflow) to use for drying. Using the effect of the temperature-controlled airflow within the tunnel, so-called direct airflow drying is achieved. Therefore, at the same time of the progress of the materials to be dried, the flow of the hot air current is also managed. Due to the evaporation of moisture, the difference in partial gas pressures towards the end of the transport is lower, which also results in a decrease of drying speed. In the high frequency electric area, the drying material acts as a dielectric object, which results in a production of heat. This is added to the flowing air current, counter-balancing the heat extraction from evaporation. This causes the loss in temperature to be reduced towards the end of the tunnel.

4. Microwave part of the machine

During traditional heat transmission, contact heat transmission, convection and radiation are present, however, heat and energy within the material can only be led inside via heat transmission (Fig. 5).

Most biological materials are quite bad at heat transmission, which causes a significant loss in energy during heat transmission processes, and due to the imbalanced water content within the material, local overheating is possible (Chen et al., 2017.).

Finally, the relative moisture content of the drying context, its temperature, and the velocity of flow determines the speed of drying.

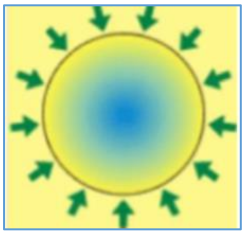

Figure 5. Flow happens from the outside towards the inside during convective heating

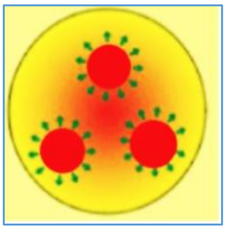

Figure 6. Microwave heats the entire mass of the material, both inside and outside

Most biological materials within an alternate current electric pressure field act as an electric agent with high loss coefficient. The (estimated) dielectric constant of the material is basically determined by the moisture content, meaning it depends on how much water there is in the material. However, ion structure is also important, which is determined by salt content. (Kurják-Bessenyei, 2014), (Kurják et al., 2012). The latter affects the specific heat of the base materials, as such, should be taken into consideration during microwave treatment as a special attribute. The energy of the microwave field affects the entire mass (Fig. 6), meaning the heat effect is higher for parts with greater internal moisture content (dielectric area), where it's the most intensive. Therefore, the effect of the microwave field is highly significant.

Sources have differing opinions on the non-thermic effects of microwaves. The theoretic explanation of non-thermic correlations is complicated, as microwave treatments are always followed by heat.

Heat transfer and moisture reduction for foodstuffs using microwave radiation is generally done at the ~2,5GHz frequency.

Due to the effects of the electromagnetic field, positive and negative potentials are biased (Fig. 7). Therefore, the effect of interaction between the electromagnetic field and the material is polarisation (Ludányi L. 2004), (Parviz, 2016).

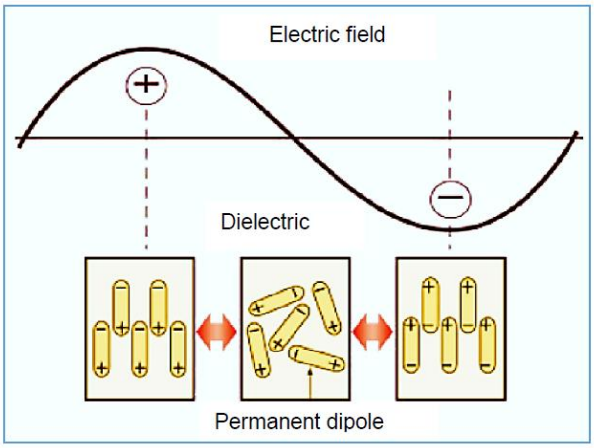

Figure 7. Molecule movements affected by shifting context

All parts of the material that became polarised seems as if one side became the positive pole, and the other became the negative pole. The electric field "organises" these dipoles, and deforms the molecule without the dipole's moment changing. In spite of the heat movement, they aim to rotate into the area. This also includes molecules which are equivalent, or have ion connection. Polar materials polarise not only by deforming, but also by orientation due to the effects of the electric field. The permittivity of dielectric agents (charge movement, rearrangement of dipoles) depends on frequency (Szabó 2005). We can calculate the transformation of microwave energy into heat within the material with relatively high precision:

$$P_D = 55{,}61 \cdot 10^{14} \cdot E^2 \cdot f' \cdot \varepsilon' \cdot tan\delta \quad (\text{W/cm}^2)$$

Where:

P_D – dissipated energy (consumed by material) [W/cm^2]
E – strength of electric field [V/cm]
f' – frequency [Hz]
ε' – dielectric constant
$\tan\delta$ – tangent of loss

Energy diffusion, and charge movement are affected by the penetration depth of the microwaves (taken for the material's sub-surface depth). Therefore, it has no effect where the energy is reduced to e^{-1} value when compared to penetration energy.

Magnetrons are the base units of microwave ovens. These transform injected direct current into microwaves with relatively high efficiency (Ludányi, 2004). The geometric shape of the wave generated within the cavity resonator affects the diffusion of the created electric field. Therefore, the structure and geometry of the handling area has to match the wavelength. Metal stirring fittings and reflective surfaces built into the handling area prevent static waves from being generated, which makes the diffusion of energy within the area more balanced (Ludányi, 2004).

Several literature sources show that microwave drying has significantly shorter duration when compared to convective drying (Kurják-Bessenyei, 2014.). Machines may be better utilised, since the amount of dried material created in one unit of time is much larger (Fig. 8).

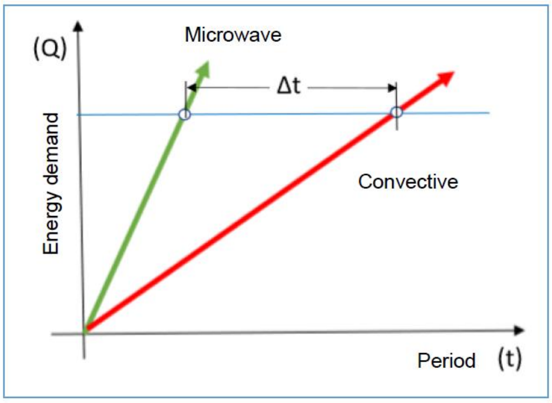

Figure 8. Microwave treatment needs less time even for identical energy input.

During dehydration using microwaves, we obtain similar velocity curves to those of convective drying, however, they show a much more intense growing trend. *Microwave drying helps the natural moisture movement within the product, which causes energy utilisation to become more efficient* (Kurják- Bessenyei, 2014), (Ludányi, 2004).

In order to protect performance measurement units, the probes give the microwave signs into the devices through fixed value absorbers. The analogue outgoing signals kept in line with measured performance reach the measurement computer through the interface.

Measured data:

$$P_d = P_h - P_v$$

Where:

P_v – performance reflecting from the material
P_d – performance dissipating in the material
P_h – input performance

From the analysis of processes, we can state that microwave drying requires roughly one magnitude less energy compared to the convective method. There are significant differences in energy consumption depending on the type of product used as material.

5. Structure of the machinery

The framework of the machinery we developed was constructed of stainless and anti-acid closed sections. This framework holds the construct, which is a tunnel-like channel (Fig. 9).

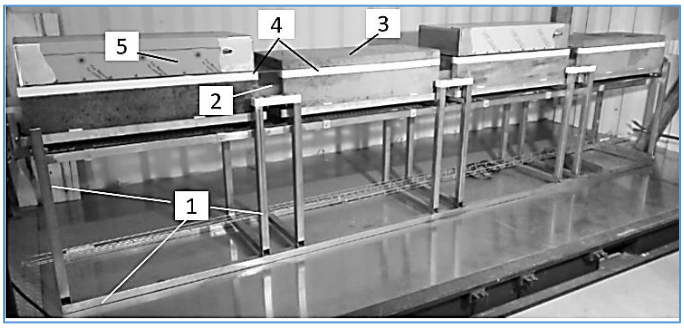

Figure 9. Side-view of the tunnel system (self-made photograph)

Explanation of abbreviations on the figure:
1. *Framework*
2. *Drying tunnel channel*
3. *High voltage / direct current panels of drying tunnel (lid)*
4. *Extension fitting (insulator)*
5. *Magnetron house*

The reflective plates under the microwave connection of magnetrons were made out of stainless and anti-acid material, and are fitted onto the lid. Therefore, in the area beneath these panels, directional plates help (increase homogeneity) the injection of radiation towards the material moving on the conveyor belt (Fig. 10).

Figure 11 shows the high voltage panel's location (in cross-section).

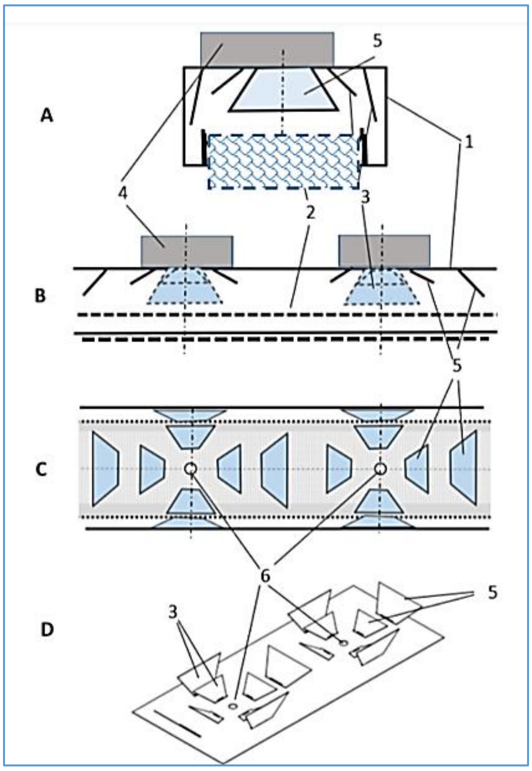

Figure 10. One part of the drying tunnel with magnetrons and reflective plates

Explanation of abbreviations on the figure:
A – cross-section,
B – longitudinal section,
C – from above,
D – axonometric sketch,
1 – internal division walls of tunnel,
2 – tunnel and perforated conveyor belt,
3 – side reflective plates to guide microwaves,
4 – magnetrons,
5 – longitudinal reflective plates,
6 – intake openings of the tunnel for magnetrons

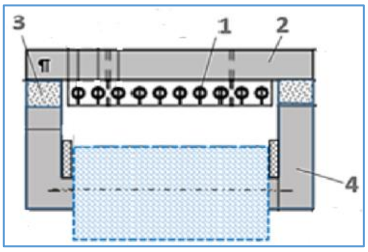

Figure 11. Cross-section of juxtalinear, alternating polarity, high-voltage unit

Explanation of abbreviations on the figure:
1- alternating polarity, high-voltage cables,
2 - lid,
3 - insulation,
4 - tunnel element.

On the top side of the tunnel, flowing air is blocked several times. These blocks tighten the bottleneck of the tunnel, and the velocity of the airflow changes. The characteristics of the airflow are shown on Figure 12, based on the ANSIS modelling.

Due to the microwave reflector, airflow increases, and air pressure decreases. Because of this phenomenon, the part below and above the perforated conveyor belt also have differing pressure levels.

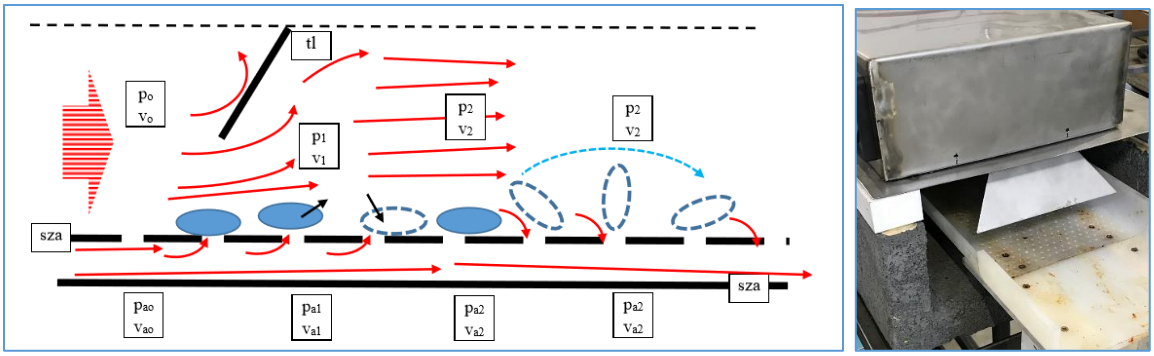

Figure 12. Changes in air pressure and velocity at the first cross-block (model and experimental device).

The figure shows (Fig. 13) the practical structure of the tunnel, where the completed material leaves the tunnel.

Explanation of abbreviations on the figure:
1 – conveyor belt,
2 – inverter motor,
3 – microwave reflector plate,
4 – Magnetron house,
5 – high voltage panel,
6 – framework structure,

Figure 13. Tunnel end, dehydrating apple

5.1. Theoretical structuring of the measurement system

The placement of the measurement units serves to determine the system's performance and energetic parameters. According to the structure seen on Figure 14, input- and output physical and energetic factors must be measured.

5.2. Pressure decrease considered for material transport

As the energy content and physical attributes of the atmosphere inside the tunnel both change, we also considered all values in linear relation, resulting in:

$$\Delta p_{v\ddot{o}} = (R_{h1} + R_{h2})Q^2$$

Calculating the resistance of the tunnel via **friction** and **shape factor** losses ($R_{h1} + R_{h2} = R_h$):

$$R_h = \frac{8\rho\lambda}{\pi^2}\frac{\Sigma 1 + \Sigma 1'}{d_e^5}$$

Meaning:

$$\Delta p_{v\ddot{o}} = R_h Q^2$$

where:

Q – intake volume flow (m^3/s)

Meaning:

$$Q = \frac{d_e^2 \pi}{4} v_1$$

v_1 – airflow velocity at intake (m/s)
d_e – equivalent flow radius (m)

When measuring for the experimental machine, $\Delta p_{v\ddot{o}}$ = 2009,88 Pa value was measured, which is almost identical to the value calculated by the flow resistance values. The smaller difference can also be caused by the significant change in vapour density expelled by the dipolar heat (but could also be due to friction resistance values). We accepted the value at 2000,0 Pa, which was validated closely by measurements (Fig. 15).

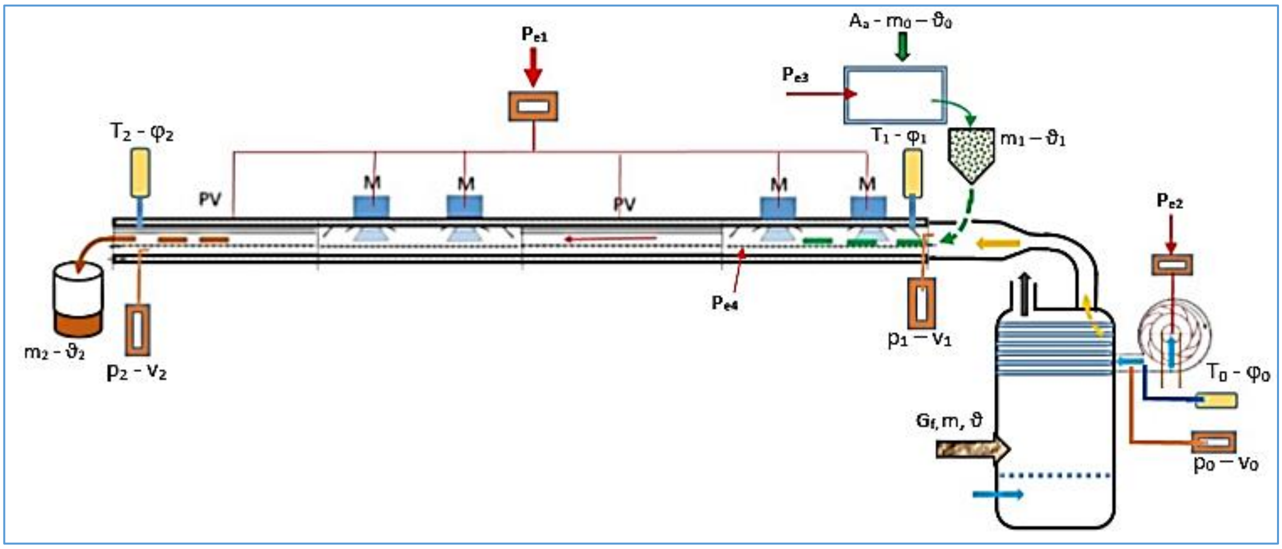

Figure 14. Structure schematics of the measurement system

Explanation of abbreviations on the figure:

Heat energy production
m – mass of wood (kg)
ϑ – its moisture content (%)
G_r – its specific energy content (MJ/kg)
P_{e2} – performance of the radial ventilator's electric engine (kW)
T_o – temperature of air intake (ºC)
φ_o – its moisture content (%)
p_o – pressure (Pa)

v_o – velocity (m/s)

Intake side of the tunnel:
P_{e4} – performance of the material transport electric engine (kW)
T_1 – temperature of drying airflow (ºC)
φ_1 – its moisture content (%)
p_1 – pressure (Pa)
v_1 – velocity (m/s)
v_2 – velocity (m/s)

Material to be dried
m_o – mass of input material before dicing (kg)
ϑ_o – its moisture content (%)
m_1 – its mass after dicing (kg)
ϑ_1 – its moisture content (%)

size of pieces (mm x mm)
P_{e3} – electric performance of dicer (kW)
P_{e1} – performance requirement of magnetrons and high voltage units (kW)

Dried material leaving tunnel:
m_2 – dried material's mass (kg)
ϑ_2 – its moisture content (%)

vapour-saturated air leaving tunnel:
T_2 – temperature (ºC)
φ_2 – moisture content (%)
p_2 – pressure (Pa)

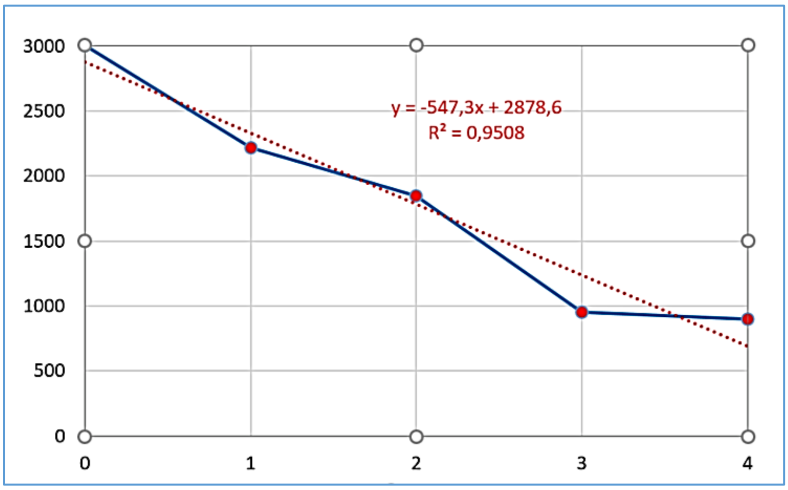

Figure 15. Pressure changes (Pa) along the length of the tunnel

It was obvious that the greatest decrease in velocity was during the part where the microwave reflection panels were placed at several different angles. In this part, the microwave changes on a scale from vertical to horizontal, due to the high frequency of reflections.

Keeping the initial velocity of the airflow constant, and merely changing load (volume passing through in time unit), a significant decrease in airflow speed was observable within the tunnel. The reason is partially the larger resistance caused by the material, and partially the more intensive evaporation of capillary water due to the microwave's effects (Fig. 16). These caused an increase in moisture content, which also caused an increase in specific density, and a decrease in temperature (Kurják. 2004).

The various dried products were analysed in the laboratory of the Institute of Horticulture, at the Hungarian University of Agriculture and Life Sciences (MATE). We determined the amount of mixtures significant for various qualities of foodstuffs (mg/100g) prior and post dehydration. Measurements were usually conducted with four repeats, in order to reduce the measurement errors, and the natural differences within the materials as much as possible. After the dehydration process, the materials were placed into inert gas environments, packed into foils, in order to dismiss any changes for the duration of the analysis (Fig. 17).

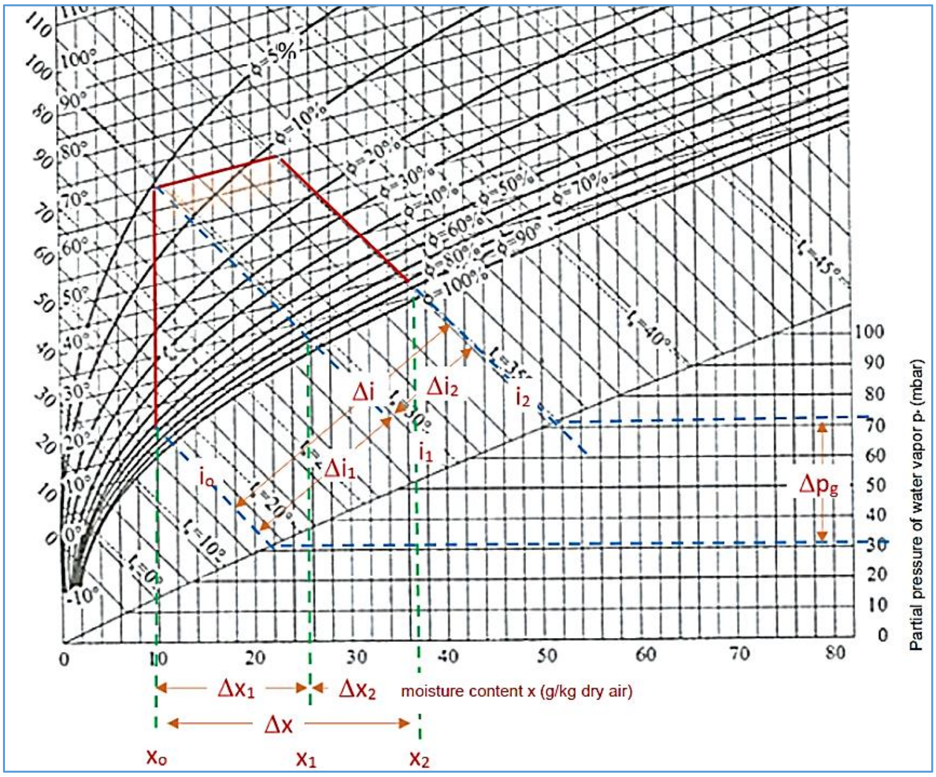

Figure 16. Edited i-x diagram, convective and microwave dehydration

Figure 17. Tomatoes prior and post dehydration process (Vertes species, top: Cukorfalat, bottom: Biborka)

Results obtained from four tomato products before (raw) and after dehydration process can be seen on Figures 18 and 19.

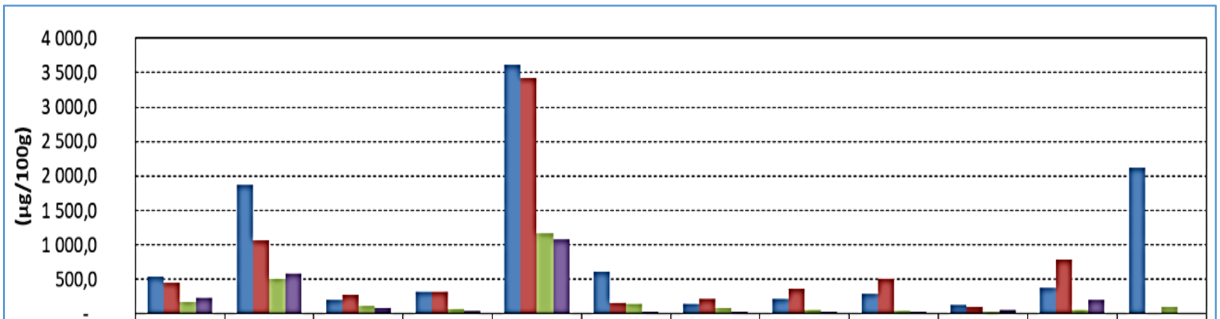

	Procyanidin B1	OH-benzoic acid	OH-cinamic acid	Procyanidin B2	Phenolic acid	Comaric acid	coffeic acid	Chlorogenic acid	Folic acid	Quercetin di-glucoside	Rutin	di-comaroyl quinic acid
BIBOR NY	543,4	1 881,2	204,1	323,7	3 616,3	616,0	142,5	218,8	297,9	130,6	374,2	2 117,5
CUK NY	451,0	1 063,6	282,0	315,8	3 419,8	163,8	218,9	369,5	512,7	109,4	791,1	-
PK NY	178,9	512,9	122,8	78,8	1 174,6	141,2	86,7	54,9	39,0	28,9	55,3	106,0
PO NY	236,9	587,0	94,7	40,3	1 079,5	35,1	35,1	32,1	24,3	52,8	197,6	-

Figure 18. Raw tomato mixtures prior to dehydration. (MATE laboratory, 2019)

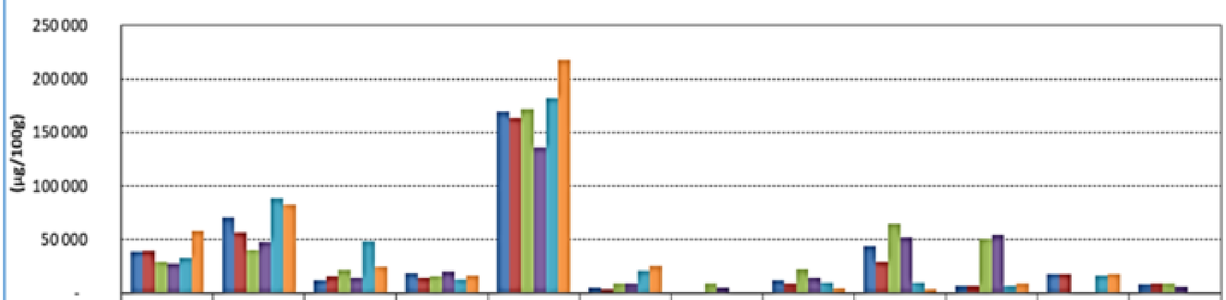

	Procyanidin B1	OH-benzoic acid	OH-cinamic acid	Procyanidin B2	Phenolic acid	Coumaric acid	coffeic acid	Chlorogenic acid	Folic acid	Quercetin di-glucoside	Rutin	di-coumaroyl quinic acid
BF ASZ	39 116	70 515	12 142	18 372	169 951	5 133	-	11 717	44 001	6 584	18 160	8 390
BKR ASZ	39 341	56 407	16 024	14 040	163 912	3 919	-	9 228	28 972	6 499	17 711	9 277
CF ASZ	29 325	40 109	21 402	15 680	171 989	9 188	9 243	22 393	64 922	50 837	-	8 858
CF ASZ	27 533	47 440	14 064	19 960	135 990	9 034	5 626	14 226	51 821	54 418	-	6 275
PK ASZ	32 865	88 244	48 645	12 764	182 016	21 257	-	9 448	10 000	7 035	16 181	-
PO ASZ	58 417	82 272	24 552	16 185	217 832	25 648	-	4 881	4 183	9 163	17 978	-

Figure 19. Mixtures of the dried tomatoes (Biborka and Cukorfalat repeat results in the top four rows, MATE laboratory, 2019)

Most important conclusions (and many more to list, but unlisted):

Among the dried tomatoes, the PO-ASZ species holds the highest lycopene concentration. The lowest concentration can be found in Cukorfalat. In spite of this, the Cukorfalat species showed a mere 4% (non-significant) loss in lycopene after processing. The loss for the PO-ASZ species was 37% during processing. The PK-ASZ species showed less degradation of lycopene at 15%. The content increased for beta-carotene – the most important source material of A-vitamin – in dried Cukorfalat and Biborka species, similarly to the first mixtures of fitoene, fitofluene and carotenoids' bio-synthesis. This proves that carotenoid's bio-synthesis continued to happen during the dehydration process of these two tomato species. The Cukorfalat and Biborka species are applicable to creating highly bioactive mixture content dried tomato products, which are important for modern and healthy diets. Price calculation: Table 1.

Table 1. Prices after dehydration, based on Auchan prices*

Name	Euro/kg	Note
Veres material (Biborka) - raw material price (Auchan)	7,71	Moisture content 88%
Energy price	0,76	Calculated
Processing price (wage, amortisation, operation)	0,55	Calculated
Total	9,03	Moisture content 20-25%
Dried (*Biborka veresi*)	36,10	Calculated

**380 HUF/Euro.*

6. Evaluation

In order to create an end product with sufficient moisture content, and keep the drying temperature between 50 and 60 centigrade at the same time, the energy amount reaching the material has to be managed. This necessitates an PLC-driven system, which optimises the energy of the microwave field, the speed of the conveyor belt, and the temperature and volume flow of the air current. Naturally, as different materials necessitate different technical parameters, experiments are necessary to determine them. The moisture content of materials to be dried has to be determined pre-dehydration, the type of material and the size of dicing also has to be accounted for. The desired end product's moisture content has to be defined. Using these data sets, the PLC controller can manage the process. The experiments validated data already present in literature, where microwave dehydration requires up to 40-70% less energy compared to conductive dehydration. The process of dehydration is significantly reduced in time.

During a gentler – low temperature – dehydration, valuable vitamins and minerals don't degrade significantly, neither in quality, nor in quantity.

The production costs and specific prices are advantageous according to calculation, much better than what was produced with traditional methods, and obtainable from the market. We may assume that final products will obtain positive reception on the market due to likeable taste and high nutrient content.

The developed small-industry and "laboratory" machinery's fundamental goal was to prove the concept of application.

Acknowledgement

The research was aided by the contract project „Megújuló energiaforrásokon alapuló és mikrohullámú anyagkezelési eljárással támogatott egyedi aszalási, szárítási berendezés kifejlesztése", ID. GINOP-2.1.2-8-1-4-16-2017-00315.

References

[1] **Aboltins A., Palabinskis J.**, (2018) Fruit Drying Process Investigation in Infrared Film Dryer. Agronomy Research 14 (1), 5–13, 2018

[2] **Beke J.**, (1997) Terményszárítás. Agroinform Budapest ISBN 983 502 646 3, 419 p

[3] **Beke, J.**, (1999) The Impact of Field Polarization on the Dewatering Process of Corn. Drying Technology, 17 (4) 687-699. p.

[4] **Beke, J., Mujumdar, A. S., Giroux M. S.**, (1997) Fundamental Attributes of Corn and Potato Drying in Microwave Fields. Drying Technology, 15 (1), 241-252.

[5] **Beke, J., Mujumdar, A.**, 1997 Hygrothermal properties of grains. In: Drying Technology in Agriculture and Food Sciences. Edited by A.S. Mujumdar. Science Publisher Inc., Enfield (NH), USA, 107-132. p.

[6] **Chen W., at al.**, (2017) Trends of spray drying: A critical review on drying of fruit and vegetable juices. Trends in Food Science & Technology Volume 65, July 2017, Pages 49-67

[7] **Dévay A.**, (2013) A gyógyszertechnológia alapjai, Pécsi Tudományegyetem Downloaded at 2016. https://www.tankonyvtar.hu/hu/tartalom/tamop412A/2011-0016_02

[8] **Moreno F.L., et al.**, (2018) Mathematical modelling of convective drying of fruits. A review Journal of Food Engineering Volume 223, April 2018, Pages 152-167

[9] **Saravacos G. D., et al.** (1999) Microwave/vacuum drying of model fruit gels. Journal of Food Engineering Volume 39, Issue 2, February 1999, Pages 117-122

[10] **Kurják Z., Bessenyei K.**, (2014) Morfológiai hatások a száradási folyamatban konvektív és mikrohullámú energiaközlés esetén, SZIE GEK Mezőgazdasági Technika, 6. sz.

[11] **Kurják Z., Barhács, A., Beke J.**, (2012) Energetic Analysis of Drying Biological Materials with High Moisture Content by Using Microwave Energy. Drying Technology 2012, 30 (3), 312-319.

[12] **Ludányi, L.**, (2004) Multimódusú mikrohullámú terek alkalmazása a szárításban. Doktori értekezés, SZIE. 153p.

[13] **Miller G., et al.**, (2012) Modeling heat and mass transfer process during convection drying of fruit. In Gu, Y T & Saha, S (Eds.) *Proceedings of the 4th International Conference on Computational Methods.* Queensland University of Technology, Australia, pp. 1-8.

[14] **Janowicz M., Lenart A.**, (2018) The impact of high pressure and drying processing on internal structure and quality of fruit. *European Food Research and Technology,* Volume 244, pages 1329–1340

[15] **Parviz A. Moghaddam, et al.**, (2016) Novel hybridized drying methods for processing of apple fruit: Energy conservation approach. Energy, Volume 103, 15 May 2016, Pages 679-687.

[16] **Radu A., et al.**, (2018) Insights in convective drying of fruit by coupled modeling of fruit drying, deformation, quality evolution and convective exchange with the airflow. Applied Thermal Engineering Volume 129, 25 January 2018, Pages 1026-1038

[17] **Szabó, G.**, (2005) Élelmiszerek minősége és a kombinált energiaközléses műveletek. Akadémiai doktori értekezés tézisei, 32p.